Coupling Renewable Energy and Storage Technologies with Hydrogen-Based Steel Production: A Design and Scheduling Optimization Approach

Carlos Prieto[a], Antonio Sánchez[a], Mariano Martín[a,*]

[a]*Department of Chemical Engineering, University of Salamanca, 37008 Salamanca, Spain*

Abstract

The decarbonization of energy-intensive industries is essential to achieve global greenhouse gas emission reduction targets. Steel production, responsible for approximately 7% of global CO_2 emissions, requires innovative low-carbon alternatives. One promising option is the use of renewable electricity and green hydrogen in the Direct Reduced Iron (DRI) process. In this study, an integrated energy system to supply renewable electricity and hydrogen to a DRI-based steel plant is analyzed. The proposed network combines two renewable power generation technologies (solar photovoltaic and onshore wind) with three complementary storage solutions (batteries, compressed hydrogen, and Liquid Organic Hydrogen Carriers (LOHCs)). A mathematical optimization framework is developed to determine both the optimal sizing and operational strategy of the system. The methodology is applied to the provinces of mainland Spain as a case study. Results highlight the critical role of integrating multiple generation and storage technologies to ensure a continuous supply of electricity and hydrogen. They also reveal a strong dependence on geographical location for design and technology selection, driven by variations in renewable resource availability. The energy cost per ton of steel is estimated at 500–600 €/t. It exceeds five fold current costs but is expected to decline significantly with future technology improvements. Hence, these integrated renewable systems are regarded to be a technically feasible and economically competitive option in the future. Overall, it represents a key enabler for the deep decarbonization of the steel sector.

Keywords: Energy storage, Decarbonization, Green steel, Hydrogen, LOHCs, Optimization.

---

*Corresponding author
Email address: mariano.m3@usal.es (Mariano Martín)

1. Introduction

The reduction of greenhouse gas (GHG) emissions has been established as one of the primary global objectives to mitigate the impacts of climate change (Allen et al., 2018). In this context, increasing the use of renewable energy sources and promoting electrification have been identified as key decarbonization strategies. These strategies are already technically and economically viable for several sectors, including buildings, light-duty transportation, industrial synthesis, cooling, heat pumps, etc. (International Energy Agency, 2020). However, certain hard-to-abate sectors remain difficult to fully electrify. A significant example is steel production. It is regarded as a highly energy-intensive process that requires elevated temperatures and a chemical reducing agent. Then, direct electrification represents a challenge. This sector is responsible for approximately 7% of global GHG emissions (International Energy Agency, 2021). Traditionally, Blast Furnace (BF) technology combined with Basic Oxygen Furnace (BOF) has been the dominant steelmaking route worldwide. This process uses coke as both a fuel and reducing agent. It leads to significant process-related CO_2 emissions (Climate Action Tracker, 2024). Consequently, decarbonizing steel production has emerged as a critical priority in the broader effort to achieve deep industrial emission reduction.

At this stage, Direct Reduced Iron (DRI) using hydrogen has emerged as a promising pathway for the decarbonization of the steel industry (Jeong and Zhang, 2025). One of the key advantages of hydrogen is its ability to act as reducing agent while eliminating direct CO_2 emissions. In this approach, iron ore is reduced with hydrogen in a shaft furnace. Then, resulting solid iron is subsequently processed in an Electric Arc Furnace (EAF) to produce liquid steel (Pawelec and Fonseca, 2022). The combination of these two technologies creates new opportunities for integrating steel production with renewable energy systems. Hydrogen can be produced via water electrolysis powered by renewable electricity. Likewise, EAF power can be provided the same way. Both strategies enable a fully renewable and low-carbon steelmaking route.

The design of the DRI process has been extensively studied in recent years to assess its technical and economic feasibility under different operating conditions. In Vogl et al. (2018), a conceptual DRI process design was proposed. Hydrogen was produced via water electrolysis, and the influence of key parameters such as electricity price, hydrogen excess, and the fraction of scrap utilization in the EAF was systematically analyzed. Similarly, Rosner et al. (2023) investigated the use of both natural gas and hydrogen for different stages of the steelmaking process. The study included the shaft furnace, reformer heating, hydrogen preheating, and ladle heating. Their study also considered the option of electric hydrogen preheating, enabling a detailed techno-economic evaluation of multiple fuel configurations for steel production. Furthermore, Immonen et al.

(2025) compared various electrolysis technologies (solid oxide electrolysis cell, proton exchange membrane electrolysis, and alkaline electrolysis) as well as different process configurations (recycling or not steam from the shaft furnace to electrolysis) and energy recovery strategies from EAF off-gases. Bhaskar et al. (2020) developed a mass and energy balance model for the DRI-EAF process. Electrolyzer efficiency significantly impacts energy consumption. However, although hydrogen storage was conceptually included in their flowsheet, it was not incorporated into the mass balance calculations; moreover, the dynamic operation of the electrolyzer was not considered, nor was the system operation optimized. These studies provide valuable insight into the DRI-H_2 process fundamentals. However, they focus primarily on process design and do not address the integration with variable renewable energy sources or the optimization of system operation.

The hydrogen-based DRI process requires large amounts of both electricity and hydrogen (Shahabuddin et al., 2023). However, relying exclusively on renewable energy introduces several operational challenges, as the electrification of industrial processes is closely linked to the availability and variability of renewable resources (Baldea et al., 2025). Current projections indicate that the dominant renewable generation technologies will be solar photovoltaic and wind power. Both of them present strong temporal variability. This intermittency contrasts sharply with the continuous and stationary operation that has traditionally characterized steel manufacturing processes. Hydrogen storage is another critical issue to ensure process stability. Its low volumetric energy density, challenging storage conditions, and material compatibility issues pose significant technical barriers (Rasul et al., 2022). Conventional storage methods such as compression and liquefaction require demanding operating conditions, leading to high energy consumption, increased investment, and safety concerns, including boil-off losses in the case of liquefaction (Abdin et al., 2021). In this context, Liquid Organic Hydrogen Carrier (LOHCs) systems have emerged as a promising alternative for hydrogen storage (Lin and Bagnato, 2024). These systems use aromatic organic liquids to store hydrogen through a catalytic hydrogenation reaction. Then, they release it via endothermal dehydrogenation. LOHCs offer key advantages, including ambient-condition storage and the potential reuse of existing oil infrastructure (Niermann et al., 2019). A comparative study by Narayanan et al. (2022) evaluated liquefaction, LOHCs, and compression for hydrogen storage. The hydrogen infrastructure was optimized to meet both electric and non-electric demand. Their findings suggest that while compression is more suitable for short-term storage, LOHCs and liquefaction technologies are better positioned for long-term energy storage applications. In Andersson (2021), LOHCs have been proposed for hydrogen storage in the steel production process. Several candidates were evaluated with a preliminary thermodynamic and economic analysis. Integration opportunities were identified with steel production technologies and compared against other conventional hydrogen storage options. Eveloy et al. (2024) explored the use of intercontinental LOHCs import from regions with high renewable availability. An ASPEN-based process modeling framework was employed, and LOHCs transportation costs were accounted for. Several scenarios were proposed combining different strategies: LOHCs-based hydrogen transport, on-site electrolysis production, heat integration between LOHCs and steel processes, and different electricity sources with varying carbon intensities. The results demonstrated that hydrogen import via LOHCs combined with the availability of low-cost heat can be economically competitive. It provides evidence that LOHCs may be regarded as a promising solution for steel production. However, the optimization of the on-site design and operation was not addressed. These findings indicate that effective integration of renewable hydrogen production with steel process requires a combination of storage technologies operating at different time horizons. LOHCs emerge as a strong candidate for seasonal storage and compressed hydrogen for shorter-term balancing.

Several works have addressed the integration of renewable energy with steel production through different modeling and optimization approaches. Table 1 provides a comparative summary of these works. In Elsheikh and Eveloy (2022) a stationary-based model was used to perform mass and energy balances with hourly electricity generation and price and PV generation data for Seville. The modeling was subsequently extended in Elsheikh and Eveloy (2023) to include cavern hydrogen storage, heat integration and part-load electrolysis operation among other elements. Five geographical locations with different wind and solar renewable characteristics were simulated using a case-based heuristic energy management strategy. Significant emission abatement relative to natural gas DRI-EAF was reported; however, the installed renewable and electrolysis capacities were varied parametrically rather than optimized and hydrogen storage capacity is prefixed, which may lead to suboptimal hydrogen storage configuration. At the same time, instant transitions for electrolyzer are assumed. Fuhrlaender et al. (2025) applied a heuristic-based approach with hourly time-series data for the simulation of different operating strategies for hydrogen-based steel production. A base case scenario was provided in which grid electricity supplied the steel process, the electrolyzer and the EAF. Two additional cases were then proposed in which hydrogen production was maximized and electrical load on the upstream power system was minimized, respectively. These strategies achieved a significantly lower upstream power load. However, hydrogen storage was not modeled on-site, and no design or operation optimization was performed.

Regarding optimization-based approaches, Devlin et al. (2023) carried out a linear programming (LP) optimization with hourly data resolution to determine the optimal capacity of a DRI steel plant coupled with hydrogen electrolysis, batteries and compressed hydrogen storage. The optimization outputs were subsequently processed with Machine Learning techniques to extend the cost assessment to over 300 locations worldwide. Nevertheless, their formulation omitted binaries and as a consequence technology selection decisions and operational constraints such as mode transitions were not captured. As a result, costs had to be represented using fixed parameters, limiting the models' ability to reflect discrete choices and operational flexibility. Similarly, Toktarova et al. (2021) employed LP optimization to size the steel process, electrolyzer, and compressed hydrogen storage equipment, analyzing the influence of hourly electricity prices on investment. However, binary variables were also omitted in their formulation, ignoring technology selection and operation mode constraints. Dautel et al. (2024) formulated a mixed-integer linear programming (MILP) model to optimize a hydrogen supply chain. They used battery and compressed hydrogen as storage technologies. Binaries were only introduced in the formulation to decide the transportation mode. However, neither operational modes nor storage selection were addressed. Finally, Stolte et al. (2026) proposed the use of medium-grade iron ore to produce green steel. They combined Genetic Algorithm (GA) with MILP optimization. An optimization loop was proposed where GA was used to set equipment capacity and MILP to optimize hourly dispatch. However, global optimality is not ensured due to the non-simultaneous nature of the optimization, and no technology selection is performed.

In the case of renewable-based industrial processes, it is essential to analyze both design and operation, since operational behavior plays a critical role in the correct sizing of units and to capture the dynamics of storage systems. The use of a MILP optimization has been widely adopted for this type of system. It enables the simultaneous optimization of process design and operation, while rigorously accounting for technical and operational constraints. Moreover, MILP provides solutions within an optimality gap under linear assumptions. Numerous studies in the literature demonstrate the effectiveness of MILP-based approaches for similar applications. Zhang et al. (2015) evaluated the operation of air separation by cryogenic distillation using a MILP optimization framework. They explored its interaction with the grid since the process is highly sensitive to fluctuations in electricity prices. 10-20% cost reductions were achieved. Similar approaches have been applied to other Power-to-X processes. In the case of ammonia production, Allman et al. (2019) analyzed wind power generation and ammonia synthesis coupling. A methodology was proposed that reduces computation time for simultaneous design and operation problems. For methanol, Svitnič and Sundmacher

Table 1: Comparative summary of existing studies on renewable energy integration with steel production

Work	Methodology	Strength/Uniqueness	Limitations
Elsheikh and Eveloy (2022)	Hourly operating strategy and sizing methodology.	Dynamic operation with hourly data from electricity market and PV pannels as energy source.	No hydrogen storage considered. Sizing and operation were done for a single location and were not optimized.
Elsheikh and Eveloy (2023)	Hourly operating strategy and sizing methodology.	Dynamic operation with hourly data from electricity market and PV/WTs as energy source. Five locations analyzed.	Sizing and operation were not optimized. Cavern hydrogen storage prefixed.
Devlin et al. (2023)	LP optimization (hourly data) + Machine Learning.	Assessment of energy and steel production cost for multiple locations. Accounted for iron ore availability. Battery and compressed hydrogen storage.	LP formulation: No technology decision nor operating mode constraints. No long-term hydrogen storage technology.
Fuhrlaender et al. (2025)	Time-series heuristic simulation.	Use of alternative energy management strategies to operate steel production plants and integration with upstream power generation systems.	Hydrogen storage not modeled. No plant design nor operation optimization.
Toktarova et al. (2021)	LP optimization (hourly data).	Electricity price analysis for two locations.	Other energy storage or long-term hydrogen storage options are not considered. LP formulation: No technology decision nor operating mode constraints.
Dautel et al. (2024)	MILP optimization (hourly data).	Supply chain optimization. Transport mode selection. Compressed hydrogen and battery storage.	No long-term hydrogen storage. No technology decision in the optimization nor operating mode constraints.
Stolte et al. (2026)	MILP optimization (hourly data).	Two-stage design and operation optimization. Compressed hydrogen and battery storage.	No long-term hydrogen storage. Global optimality is not ensured (non-simultaneous optimization).

(2022) examined an integrated process configuration that includes waste heat recovery and energy storage systems, such as thermal storage and LOHCs systems. In the process industry, operational flexibility has also been studied in more traditional sectors. For example, Germscheid et al. (2023) investigated copper production under uncertain electricity prices using stochastic programming. The economic advantages of participating in the intraday electricity market were highlighted and 2–6% profit increase was reported.

Despite these advances, several gaps remain in the literature regarding the optimal design and operation of renewable energy systems for green steel production. As summarized in Table 1, three main limitations can be identified. First, to the best of the authors' knowledge, no MILP formulation has been proposed that simultaneously optimizes process design and operation for this application. The introduction of binary variables for technology selection and for enforcing operational constraints (such as mode transitions) is essential to capture the discrete nature of these decisions. Second, most of the existing studies predominantly rely on short-term storage technologies such as compressed hydrogen or batteries or in cavern hydrogen storage that may be unavailable. Other long-term alternatives such as LOHCs are generally not considered. As demonstrated in Narayanan et al. (2022) and Eveloy et al. (2024), different storage technologies serve complementary roles at distinct time horizons, and their combination can improve both reliability and cost-effectiveness. Third, although geographical variability is sometimes considered, studies either use LP formulations, leading to suboptimal technology dispatch, or apply MILP without simultaneous optimization of process design and operation.

Therefore, in this work, the design and scheduling optimization of an integrated energy system that supplies green electricity and hydrogen to a DRI alternative steel production plant is evaluated. The proposed installation integrates solar photovoltaic and onshore wind power as the primary renewable electricity sources. These are combined with multiple energy storage technologies to ensure a reliable supply. Batteries are included to balance, mainly, daily power fluctuations; however, their limited capacity to address seasonal variability requires complementary long-term storage solutions. Hydrogen plays a dual role in the system. First as a feedstock for the DRI steelmaking process. Additionally as an energy storage solution coupled with a fuel cell to produce electricity during periods of low renewable generation (Griffiths et al., 2021). For hydrogen storage, both compression and LOHCs systems are evaluated. These correspond to short-term and long-term storage horizons, respectively. Although large-scale hydrogen liquefaction could serve as another alternative, its high capital cost, complex operating conditions, and significant energy inefficiencies make it less attractive in this context. Furthermore, LOHCs systems offer the additional advantage of reusing existing liquid fuel infrastructure. Consequently, liquefaction is excluded from the scope of this study.

The remainder of this paper is organized as follows. Section 2 describes the energy generation and hydrogen storage systems considered, as well as the mathematical formulation used for the optimization framework. Section 3 outlines the steel production requirements and their integration with the proposed energy system. Section 4 presents and discusses the main results of the design and scheduling analysis, including technical and economic assessments. Finally, Section 5 summarizes the key conclusions.

2. Process description and model formulation

In this section, steel production process and energy and hydrogen production and storage systems are introduced. Then, the MILP model is formulated for optimal design and scheduling.

2.1. Process description

The production of DRI with hydrogen has been proposed as a key pathway for decarbonizing the steel sector. In this process, iron ore is fed to a shaft furnace, where hydrogen acts as the reducing agent to produce sponge iron. The resulting product is then transferred to an EAF, where is melted using electricity. In some cases, scrap metal can also be added to the EAF, reducing the demand for primary iron ore. The main outputs of the process are liquid steel and slag (Vogl et al., 2018; Rosner et al., 2023). This production route requires large amounts of renewable electricity and hydrogen, which must be supplied reliably to ensure continuous operation. Since steel manufacturing typically operates under steady-state conditions, the integration of renewable energy sources must be carefully designed to guarantee a stable supply for the alternative DRI–EAF steelmaking process.

This work proposes an integrated, self-sufficient energy system designed to supply both the electricity and hydrogen required for the steelmaking process (the general scheme is depicted in Figure 1). The system integrates two primary renewable energy sources: photovoltaic solar and onshore wind. To support renewable generation, several energy storage technologies are incorporated. These include battery systems and hydrogen storage through compression and LOHCs. While batteries and compressed hydrogen are well suited for short to medium-term storage, LOHCs technology is particularly advantageous for long-term energy storage. Compression and battery systems have been already identified as reliable solutions for integrating renewables into industrial operations (Schrotenboer et al., 2022). The rationale for combining these three storage technologies is based on their complementary operational characteristics. Batteries offer high round-trip efficiency and fast response. However, the high associated investment and volume typically limit their capacity in industrial-scale applications (Kebede et al., 2022). Compressed hydrogen storage provides greater operational flexibility to the system, enabling fast storage and release of surplus hydrogen. Nevertheless, it requires high-cost pressure vessels that constraint its economic viability for large storage volumes, and its round-trip efficiency is reduced compared to batteries due to compression energy losses (Narayanan et al., 2022). Finally, LOHCs systems offer comparable energy density to compressed hydrogen at significantly lower storage costs and are particularly suited for seasonal energy storage, as they allow ambient storage conditions

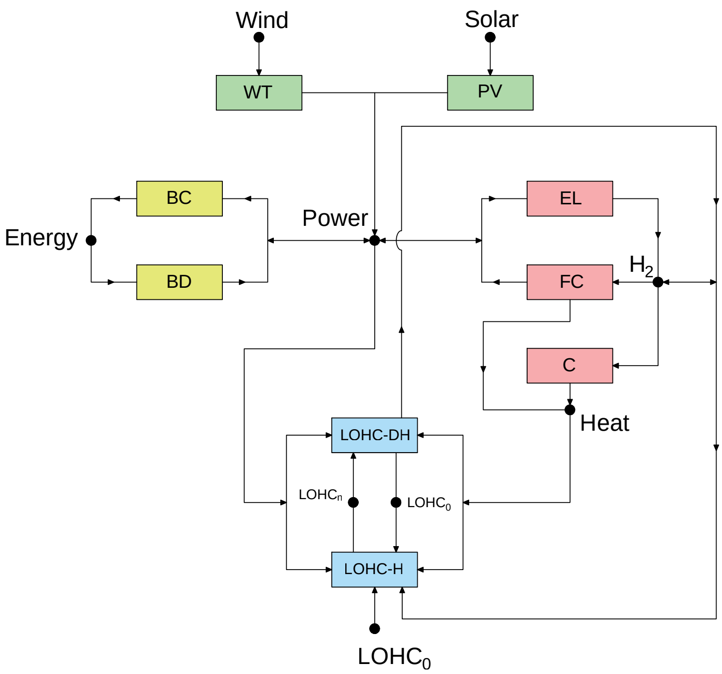

Figure 1: Energy and hydrogen storage superstructure. WT: Wind turbines; PV: Photovoltaic panels; BC: Battery charge; BD: Battery discharge; EL: Electrolyzer; FC: Fuel cell; C: Combustion; CP: Compression; DCP: Decompression; LOHC-H: LOHC hydrogenation; LOHC-DH: LOHC dehydrogenation.

and benefit from fast reactor start-up dynamics (Gambini et al., 2024; Bollmann et al., 2023). However, its overall storage efficiency is lower than compression due to thermal energy required for dehydrogenation (Prieto et al., 2025). The MILP formulation presented in Section 2.2 simultaneously optimizes the technology selection, allowing the model to include or discard a specific technology, sizing, and hourly dispatch of all three technologies, rigorously accounting for the specific operational constraints of each one.

Several LOHCs systems have been proposed in the literature (Niermann et al., 2019). In this work, two specific systems are considered: N-ethylcarbazole (LOHC1) and an indoles mixture composed by 1,2-dimethylindole with 7-ethylindole (LOHC2). The selection of these candidates is based on previous studies (Prieto et al., 2025). There, economic, environmental, and safety indicators were evaluated to identify promising hydrogen storage options. At this point, comparing LOHCs systems with different physicochemical and techno-economic characteristics (such as reaction conditions, CAPEX and OPEX, storage capacity, and raw material price) allows for a more comprehensive understanding of their potential for large-scale deployment.

Table 2: Energy and hydrogen production, storage and utilization technologies.

Technology	Input	Output
PV pannels (PV)	Solar radiation	Power
Wind turbines (WT)	Wind speed	Power
Water electrolysis (EL)	Power Water	Hydrogen Oxygen
Fuel cell (FC)	Hydrogen Air	Power Heat Water
Combustion (C)	Hydrogen Air	Heat Water
Battery Charge (BC)	Power	Energy
Battery Discharge (BD)	Energy	Power
LOHCs hydrogenation (LOHC-H)	Hydrogen LOHC-H_0 Power Heat	LOHC-H_n
LOHCs dehydrogenation (LOHC-DH)	LOHC-H_n Power Heat	LOHC-H_0 Hydrogen

The possibility of storing hydrogen and converting it back into electricity is also explored in the proposed system. For this purpose, a Solid Oxide Fuel Cell (SOFC) is incorporated into the network. This technology is particularly suitable for the integration with LOHCs based hydrogen storage. LOHCs primarily rely on thermal energy for the dehydrogenation reaction. The exhaust heat from the SOFC can be effectively integrated to supply part of that required for hydrogen release (Preuster et al., 2018). If additional heat is needed, hydrogen combustion is introduced as an additional support option. It is important to note that, unlike other resources, thermal energy is not stored in the proposed system. By combining these technologies, an integrated generation and storage superstructure for power and hydrogen is proposed. Table 2 summarizes the different technologies included in the system, detailing their respective input and output resources.

2.2. *Model formulation*

An integrated design and scheduling optimization formulation is developed to determine the optimal sizing and operation of the facility that supplies renewable electricity and hydrogen to the steel production process. The model builds upon the framework proposed by Zhang et al. (2016), incorporating the necessary modifications to address the specific characteristics of this problem. A brief overview of the modeling approach is provided here, while the complete mathematical formulation is presented in the Supporting Information. The proposed model adopts a multiscale temporal framework, in which the annual planning horizon is divided into a set of arbitrarily defined seasons. The duration of each season may vary, enabling an accurate representation of seasonal fluctuations in renewable resource availability. In this study, a one-year horizon is considered, with seasons defined on a monthly basis and an hourly time resolution within each period. Although this formulation provides flexibility in representing temporal dynamics, no temporal aggregation is applied, thereby preserving the full temporal granularity of the optimization problem. A cyclic scheduling strategy is applied within each season, while inventory carryover is allowed between seasons to capture long-term storage dynamics, which are crucial for seasonal balancing. From an operational perspective, each process unit is represented by four operating modes (off, startup, on, and shutdown) subject to minimum residence time constraints in each mode. The system must simultaneously meet two distinct demands (electricity and hydrogen) at every time by optimally coordinating the available generation and storage technologies within the network.

The model's constraints are divided into three areas.

(1) First, those relating to the material and energy balances of the different processes within the network. The basic equation for the network's operation is as follows:

$$\overline{Q}_{jht} = \overline{Q}_{jht-1} + B_{jht} - S_{jht} + \sum_{i} \rho_{ij} P_{iht} \quad \forall\, j,\, h,\, t \in \overline{T}_h \tag{1}$$

In this equation, the quantity of resource j stored at time t in season h is denoted by $\overline{Q}_{jht}$. The variables B_{jht} and S_{jht} represent the amounts of resource j consumed and discharged, respectively. The term P_{iht} denotes the production or consumption of the reference resource associated with process i. Finally, the parameter ρ_{ij} specifies the conversion factor that relates resource j to the reference resource of process i.

(2) The production of the reference resource in process i is limited by the correspond-

ing plant capacity (C_i):

$$P_{iht} = \eta_{iht} C_i \quad \forall\, i \in \{PV, WT\},\, h,\, t \in \overline{T}_h \tag{2}$$

$$P_{iht} \leq \eta_{iht} C_i \quad \forall\, i \in I \setminus \{PV, WT\},\, h,\, t \in \overline{T}_h \tag{3}$$

The parameter η_{iht} represents the time-dependent process capacity, which is particularly relevant for variable renewable technologies such as wind and solar power generation. In these cases, the effective capacity depends not only on the nominal plant size but also on resource availability. Specifically, η_{iht} is determined from solar irradiance and ambient temperature (Sánchez and Martín, 2018; Hlal et al., 2019), or from wind velocity (de la Cruz and Martín, 2016), for each time period and location. Other restrictions relating to processing and storage capacities, as well as the amount of resources introduced, have also been incorporated. See Supporting Information.

(3) Related to the mode operation constraints, each process can operate in four distinct modes: off, startup, on, and shutdown. The binary variable y_{imht} indicates whether process i is operating in mode m during season h and time period t. If a process is active, one operating mode must be assigned:

$$\sum_{m \in M_i} y_{imht} = x_i \quad \forall\, i,\, h,\, t \in \overline{T}_h \tag{4}$$

The set M_i denotes the collection of admissible operating modes for process i.

(4) Another important restriction within the proposed network is that relating to the maximum variation in capacity within the same operating mode. This maximum variation is limited by a given amount ($\bar{\Delta}_{im}^{\max}$) as shown in the following equation:

$$\begin{aligned} -\bar{\Delta}_{im}^{\max} - \overline{M}(2 - y_{imht} - y_{imh,t-1}) &\leq \overline{P}_{imht} - \overline{P}_{imh,t-1} \\ &\leq \bar{\Delta}_{im}^{\max} + \overline{M}(2 - y_{imht} - y_{imh,t-1}) \quad \forall\, i,\, m \in M_i,\, h,\, t \in \overline{T}_h \end{aligned} \tag{5}$$

The variable $\overline{P}_{imht}$ represents the amount of reference resource that is consumed or produced by process i when operating in mode m during season h and time period t. Additional restrictions in terms of feasible transitions and minimum stay time periods are also implemented.

(5) Finally, some continuity constraints are also included to ensure the feasible transition between seasons. A cyclic scheduling structure is imposed; consequently, the initial operating mode of each season must coincide with its final mode. Furthermore, the state at the end of one season must be identical to the state at the beginning of the subsequent season.

The objective of this work is to meet a given electricity and hydrogen demand ($D_{j,h,t}$) using the different proposed technologies (including storage systems).

$$S_{jht} = D_{jht} \quad \forall\, j \in \hat{J},\, h,\, t \in \overline{T}_h \tag{6}$$

The objective function of the optimization problem is defined as the total operating cost (OC) of the system:

$$\begin{aligned} OC = & \sum_i \sum_{m \in M_i} \sum_h \sum_t J_{imht} + \sum_i \sigma_i \left(\delta_i x_i + \gamma_i C_i\right) + \\ & \sigma_j \left(\overline{Q}_{LOHC_0,1,0} + \overline{Q}_{LOHC_n,1,0} \frac{MW_{LOHC_0}}{MW_{LOHC_n}}\right) C_{LOHC_0} + \\ & \sum_{j \in \hat{S}} \left(\alpha_j \bar{x}_j + \beta_j \overline{C}_j\right) + \sum_i \sum_j \sum_h \sum_t \xi_{ij} \rho_{ij} P_{iht} \end{aligned} \tag{7}$$

The objective function accounts for the operating costs of both production processes and storage. The process-related cost is divided into three components. The first term, J_{imht}, encompasses all operating expenses unrelated to capital investment, such as raw materials and utilities. The second component of Equation 7, represented by the last term in the first line of the equation, captures the operating costs associated with the initial investment, including capital charges and maintenance (Sinnott and Towler, 2019). A linear approximation of the capital cost of the processes with the proposed capacity is assumed. The LOHCs inventory is also incorporated (second line of the objective function), considering the initial storage amount of LOHCs. Likewise, the storage cost is expressed through two components. The first term (in the third line of the equation) corresponds to the amortization of capital cost, also approximated linearly. The second term reflects the operating and maintenance costs of storage, represented by the last term in the third line.

The set of equations in the model results in a mixed integer linear optimization programming problem (MILP). It has been implemented in Julia using the JuMP package and solved with Gurobi. An optimality gap of 1% is set.

3. Case Study: Steel Production

To assess the potential integration of the proposed renewable energy and hydrogen system with steel production, a representative steel manufacturing plant is selected as a case study. Specifically, the analysis focuses on the steel sector in Spain, where several BF–BOF and EAF facilities are currently in operation, producing crude steel. For the purposes of this work, a typical EAF facility is considered, with a representative production capacity adapted for hydrogen-based DRI production (Pawelec and Fonseca, 2022). Typical values for hydrogen and electricity consumption for these systems are used. In the case of electricity, the demand includes not only the Electric Arc Furnace (EAF) itself but also other auxiliary energy requirements within the plant, such as hydrogen preheating, shaft furnace operation, and iron ore heating (Yadav et al., 2021). The specific parameters and consumption values adopted are summarized in Table 3. Moreover, to simulate a more restrictive operating scenario and emphasize the importance of continuous power supply, no scrap usage in the EAF is assumed. Finally, the steel production process is modeled under steady-state operating conditions.

Table 3: Steel production energy and hydrogen requirements.

Parameter	Value	Reference
Plant capacity	$1 \cdot 10^6$ ton/y	(Pawelec and Fonseca, 2022)
Hydrogen consumption	51 kg_{H_2}/ton	(Yadav et al., 2021; Vogl et al., 2018)
Energy consumption	1.26 kWh/ton	(Yadav et al., 2021; Vogl et al., 2018)

This work evaluates the integration of an integrated electricity and hydrogen production facility with a steel manufacturing plant, based on the data presented in Table 3. The optimization model described in the previous section is applied to determine the optimal design and operational strategy of such a system. The analysis focuses on the implementation of this concept in Spain, considering all provinces of mainland Spain (48 regions in total). These regions exhibit significant spatial variability in renewable energy potential. This leads to notable differences in the cost of electricity and hydrogen generation. Assessing these variations enables to identify the locations with the most favorable energy cost profiles for steel production. Furthermore, this assessment provides valuable insight into whether existing steel production sites are located in the emerging renewable energy landscape. This allows a comparative evaluation between retrofitting existing facilities and constructing new plants in locations with lower energy costs. In addition, this formulation supports strategic planning for a cost-effective and sustainable steel sector transition.

The parameters required for the proposed model were collected from various sources. Meteorological data were obtained from public databases (Davis et al., 2023; European Commission, 2025). For the battery system, charging and discharging efficiencies, as well as cost parameters, were sourced from Gonzalez-Castellanos et al. (2020) and Allman et al. (2019). Data related to hydrogen production were based on a PEM electrolyzer, following Sánchez et al. (2022), while operational parameters for the

SOFC fuel cell were taken from Peters et al. (2016). Finally, the parameters for LOHCs systems were selected from previous work on the area (Prieto et al., 2025). For the sake of brevity, details of the parameters used were included in the Supporting Information file.

The aim of this work is to minimize the total operating costs of an integrated hydrogen and energy system to supply both resources to a typical steel mill. A broad range of scenarios is covered, as optimization is carried out across a considerable number of regions, each one considering its individual solar and wind profiles. As introduced before, the MILP formulation is solved with a 1% optimality gap, ensuring that the obtained solutions are within 1% of the global optimum. Nevertheless, several intrinsic and extrinsic factors may influence the final process design and operation, such as technological improvements, cost variations, regulatory constraints or land availability. It is not the purpose of this work to quantify their effect, but given the nature of the formulation, the model can be easily adapted for these and other situations. This would simply require including additional design or operational constraints or modifying cost and/or performance parameters.

4. Results

This section is divided into two. First, the results related to the operation of renewable energy generation and the integration with energy storage technologies are included. Then, the techno-economic analysis is presented for different case studies.

4.1. Operation Results

In this section, the operational characteristics of the proposed integrated facility for supplying green electricity and hydrogen to a steel production plant are evaluated. Although 48 provinces in Spain were analyzed in this study, for the sake of brevity, the discussion focuses on three representative locations to illustrate the performance of the system under different renewable energy conditions. The selected provinces are Córdoba, A Coruña, and Guadalajara. Córdoba was chosen due to its high solar energy potential, A Coruña for its strong wind resource, and Guadalajara as a balanced case combining both solar and wind resources. The optimized capacities for each process and storage technologies are summarized in Table 4. The scheduling results are presented for representative weeks in both summer and winter to capture seasonal variations. These results are shown for the two LOHCs systems evaluated in this work. Hence, they provide insight into their operational flexibility and integration with renewable energy availability.

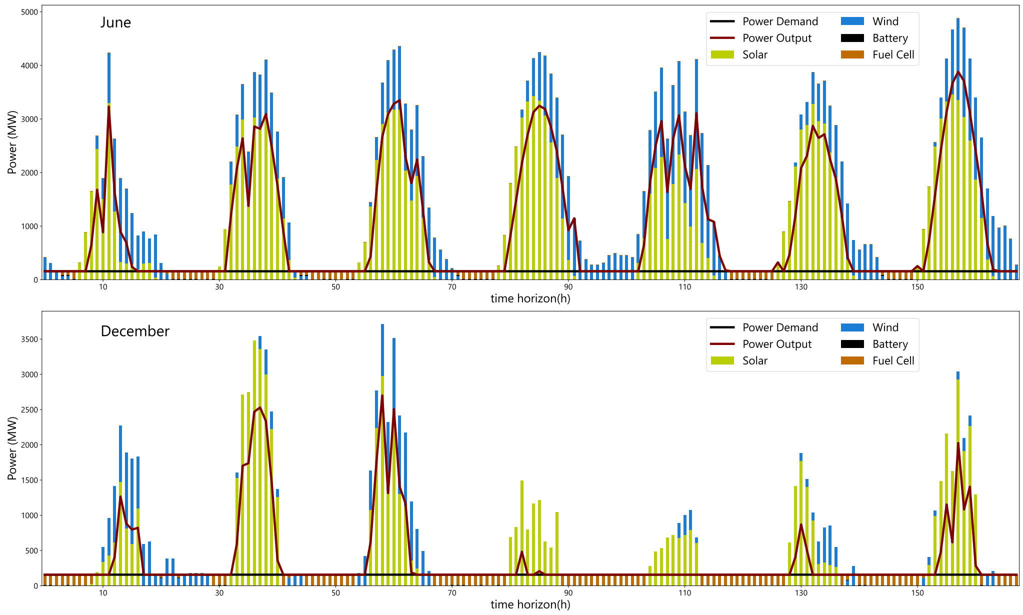

Figure 2: Electricity scheduling results in the province of Córdoba for the system with N-ethylcarbazole as LOHC

Firstly, Figure 2 shows the scheduling results for electricity production and demand when using N-ethylcarbazole as LOHC in the province of Cordoba. The figure illustrates the contributions of different energy sources: wind and solar generation, along with two electricity storage technologies, battery storage and hydrogen fuel cells. Additionally, the electricity demand profile and the total electricity output from the integrated facility are represented. In this southern Spanish location, solar energy represents the primary renewable source. This exhibits a clear diurnal pattern characterized by high renewable generation during midday and no production at night. Wind energy provides a smaller share (approximately 25%), with a more dispersed temporal distribution. During summer, solar availability is significantly higher. Peak power outputs of around 3000 MW each day and extended periods of generation are found. It is also worth highlighting that solar energy requires a larger installation area compared to wind to supply the same amount of electricity and hydrogen. Energy storage plays a crucial role in ensuring that electricity demand is met over all year. As shown in the figure, during certain hours, particularly at night, 100% of the electricity demand is covered by the storage systems. The contribution from the battery system is limited by its installed capacity of 360 GJ (100 MWh) and a maximum charge/discharge rate of 10 MW. These maximum capacities are considered based on typical values for battery systems (Kebede et al., 2022). Across all evaluated provinces, this capacity is fully utilized, highlighting that battery performance is constrained by its storage volume. Consequently, the remaining stored electricity is supplied by the stored hydrogen (compressed or LOHCs) using the fuel cell system. This technology provides greater capacity flexibility to balance generation and demand.

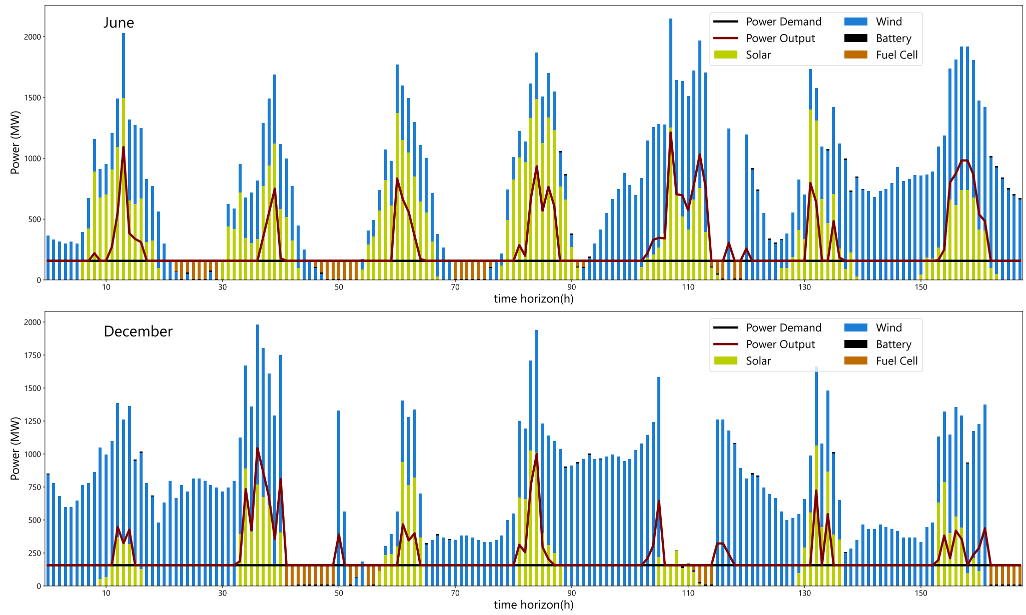

Figure 3: Electricity scheduling results in the province of A Coruña for the system with indoles mixture as LOHC

Another key aspect in the operation of these facilities is the excess electricity generation in some periods, as illustrated in Figure 2. This phenomenon is particularly pronounced during the central hours of the day, when solar power output reaches its peak. According to the optimization results, it is economically more favorable to curtail the surplus electricity produced during these periods than to store it, due to the high storage costs. In Córdoba, the total amount of electricity produced but not used on-site over the whole year is equivalent to 4.8 times the plant's electricity demand. This value is strongly influenced by the distribution of wind and solar resources in the region.

To further explore this effect, Figure 3 presents the electricity scheduling profile for A Coruña. There, wind energy accounts for approximately 56% of total electricity generation. In this location, wind power is abundant but exhibits no clear temporal pattern, unlike solar energy. The maximum power output reaches around 2000 MW in both winter and summer weeks. This is significantly lower than in Córdoba, where peak values of up to 5000 MW are reached, particularly in summer. During nighttime, when no solar generation occurs, electricity demand is met through wind generation or storage systems. Conversely, during periods with low wind availability, storage systems are required to supplement solar energy to maintain supply. As in Córdoba, electricity surplus also occurs in A Coruña. This especially found during midday when both solar and wind generation overlap. However, the magnitude of this surplus is significantly lower, approximately 1.9 times the total plant's electricity demand over the year. It is less than half the surplus observed in Córdoba. This clearly indicates a relationship between the renewable energy mix and the amount of excess electricity generated. Solar energy, with its predictable day/night cycle but high seasonal variability, demands from renewable generation capacity oversizing to ensure supply security throughout the year. In contrast, wind energy, despite being more stochastic, exhibits lower seasonal variability. In the end, it reduces curtailment. This behavior also impacts storage system sizing. As shown in Table 4, A Coruña, characterized by the highest wind availability, requires the smallest hydrogen and LOHCs storage capacities among the evaluated provinces. For example, for LOHC1, when compared with Córdoba, the hydrogen storage capacity decreases by 388%, and the LOHC storage capacity by 45%. This illustrates how the renewable energy profile directly affects infrastructure requirements and investment cost.

Table 4: Process and storage capacities for three selected provinces and the two LOHC system: N-ethylcarbazole (LOHC1) and the indoles mixture (LOHC2)

	LOHC1			LOHC2		
	Cordoba	**Coruña**	**Guadalajara**	**Cordoba**	**Coruña**	**Guadalajara**
Solar PV (km^2)	20.36	9.78	10.82	22.48	9.95	10.92
Wind Turbines (km^2)	4.37	2.87	3.46	5.43	2.86	3.75
Battery (MW)	10.00	10.00	10.00	10.00	10.00	10.00
Electrolyzer (MW)	1000.00	923.56	1000.00	1000.00	926.16	1000.00
Fuel Cell (MW)	154.11	157.19	157.19	152.92	154.22	153.80
H_2 Combustion (MW_t)	0.00	2.99	0.66	30.19	38.25	1.66
LOHC Hydro (kg H_2/s)	0.31	1.37	0.92	0.72	1.96	1.61
LOHC Deshydro (kg H_2/s)	3.01	3.89	2.74	1.36	3.19	2.86
Electricity Battery (GJ)	360.00	360.00	360.00	360.00	360.00	360.00
Hydrogen (t)	1000.00	204.88	391.82	1000.00	242.99	338.07
LOHC0 (t)	117301.42	80376.18	117242.18	118363.23	102929.84	118312.65
LOHCn (t)	123000.00	84465.72	123000.00	123000.00	107054.55	123000.00

Another essential aspect to understand and evaluate the design and operation of these facilities is the hydrogen production, consumption, and storage performance. Figure 4 illustrates the hydrogen flow in the system for the province of Guadalajara. The hydrogen produced by the electrolyzer, consumed by the fuel cell, and stored or released through the two storage alternatives (compressed hydrogen and LOHCs-based storage) are represented. The operation of the electrolyzer is strongly correlated with the availability of renewable energy. Maximum hydrogen production typically occurs during the central hours of the day. This is when solar and wind generation are the highest. The Figure 4 clearly highlights the differences between summer and winter operation. In summer, the electrolyzer operates at maximum capacity for extended periods. This is driven by the more intense solar resource, whereas in winter, its operation is significantly reduced. In both Guadalajara and Córdoba, the maximum allowed electrolyzer capacity of 1 GW is reached during these peak production periods while in A Coruña lower capacities are set. When hydrogen production can exceed immediate consumption, the surplus is stored through two distinct pathways: compression and LOHCs hydrogenation. Compressed hydrogen provides greater operational flexibility. It enables short-term balancing that closely follows the fluctuations in renewable generation. In contrast, the LOHCs storage option is better suited for seasonal energy storage. As shown in the Figure 4, hydrogenation of the LOHCs occurs primarily in summer, coinciding with high electricity generation. In winter, dehydrogenation of the LOHCs releases hydrogen to supply both the plant's hydrogen demand and power demand using fuel cell. Finally, as previously noted in the electricity scheduling results, the hydrogen fuel cell plays a crucial role in maintaining energy supply during periods of low renewable generation. This is particularly evident at night, when solar production is zero and wind availability is reduced. During the winter week presented, this effect becomes even more pronounced. Entire periods are shown where both electricity and hydrogen demand at the steel plant are fully supplied by storage systems.

To evaluate the influence of solar and wind availability on hydrogen system operation, Figure 5 presents the hydrogen scheduling results for A Coruña. Compared to Guadalajara and Córdoba, notable differences can be found. In A Coruña, where wind is the dominant renewable resource, hydrogen production via water electrolysis reaches similar peak levels in both summer and winter. This reflects the more stable seasonal wind profile. The most significant variation, however, is related to LOHCs-based storage. Unlike in the previous cases, LOHCs dehydrogenation occurs also during summer, while hydrogenation takes place also during winter. This flexible seasonal trend arises from the distinct wind and solar availability profiles in the region. To better visualize this phenomenon, Figure 6 depicts the annual storage profiles for hydrogen and LOHCs for the three selected provinces. These profiles clearly highlight the impact of resource distribution on storage behavior. As expected, compressed hydrogen storage

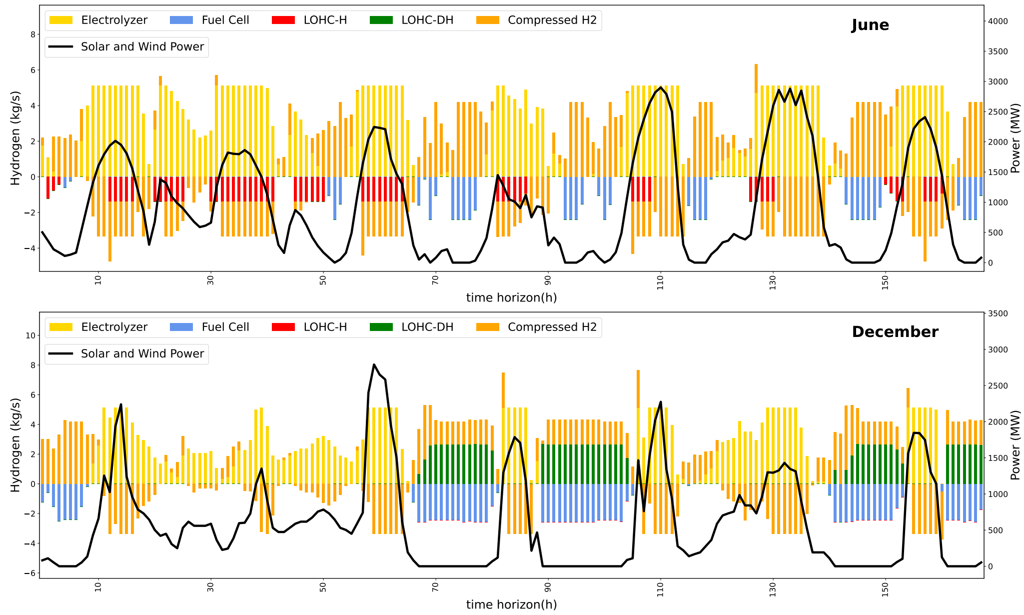

Figure 4: Hydrogen scheduling results in the province of Guadalajara for the system with N-ethylcarbazole as LOHC

exhibits more fluctuating behavior. It acts as a short-term buffer to smooth the variability in renewable generation. However, substantial differences exist between provinces. A Coruña, with the highest share of wind power, shows the most oscillatory pattern, which reflects the stochastic nature of wind energy. Storage capacity requirements are also location-dependent. For example, in Córdoba, the maximum compressed hydrogen storage capacity reaches approximately 1000 t, while in A Coruña this value is significantly lower, around 200 t. Although a clear linear trend between renewable resource mix and hydrogen storage capacity is not observed, it is notable that all locations reaching maximum hydrogen storage capacity utilization have a solar share above 65%. This indicates that high solar penetration drives larger storage requirements due to its strong diurnal and seasonal variability. In contrast, wind-dominated systems rely less on large storage volumes.

In terms of LOHC-based storage, Figure 6 clearly demonstrates that LOHCs systems enable large-scale seasonal energy storage. This is essential to address the seasonal fluctuations in solar and wind electricity production, particularly in solar-dominated regions, where seasonal differences are more pronounced. LOHCs ensures reliable energy and hydrogen storage to meet the demand in steel production. At the same time, the optimization results show that combining LOHCs for seasonal energy storage with compressed hydrogen represents the most cost-effective alternative for meeting a given

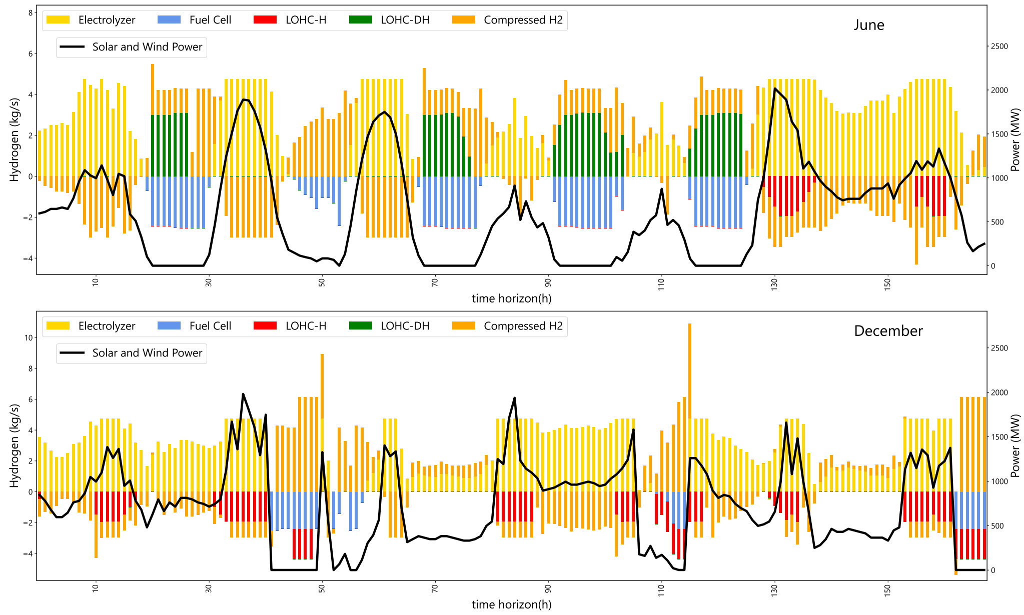

Figure 5: Hydrogen scheduling results in the province of A Coruña for the system with indoles mixture as LOHC

energy demand. As previously noted, not all excess electricity is stored due to economic constraints; nevertheless, seasonal storage technologies will play a critical role in future decarbonized energy systems. The scheduling results highlight clear variations among the selected provinces, which are strongly influenced by their respective wind and solar resource distributions. In Córdoba and Guadalajara, LOHCs storage primarily occurs during spring and summer. This is when photovoltaic generation is at its peak. In contrast, the storage profile for A Coruña shows marked differences: wind generation does not display significant seasonal variation, and therefore, the seasonal impact on storage is less pronounced. This behavior directly affects storage capacity requirements, as summarized in Table 4. Among the three provinces, A Coruña has the lowest LOHCs storage capacity. This is consistent with the less seasonal nature of wind, which reduces the need for large-scale seasonal storage. Conversely, in Córdoba and Guadalajara, the maximum LOHCn capacity proposed for the optimization of approximately 123000 t is reached in both LOHC systems, reflecting the strong seasonal character of solar energy. Interestingly, while total storage capacity is lower in A Coruña, the hydrogenation and dehydrogenation process capacities are higher. It indicates more frequent and faster uscycling due to the stochastic nature of wind. As illustrated in Figure 6, solar generation follows a predictable seasonal pattern, with high production in summer and low in winter. Wind generation, in contrast, is less predictable and lacks a regular seasonal profile, leading to more frequent and irregular fluctuations. Therefore, energy storage systems in wind-dominated regions must be designed for higher operational flexibility, whereas solar-dominated systems require larger seasonal storage capacities to balance long-term variability.

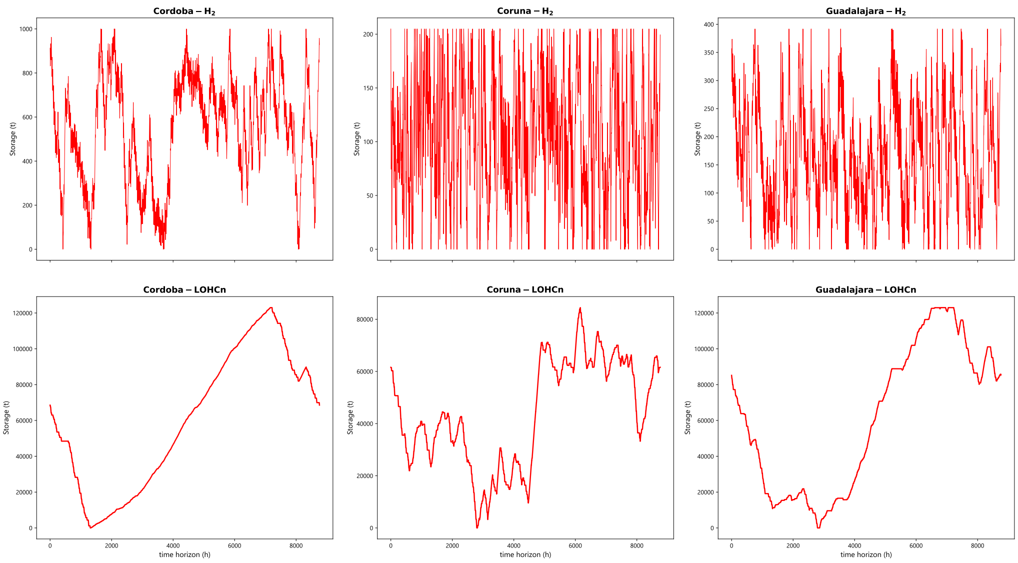

Figure 6: Yearly hydrogen and LOHCn storage profiles for the system with indoles mixture as LOHC

In hydrogenation and dehydrogenation processes, heat is a critical resource that must be carefully managed to ensure efficient system operation. Within the analyzed energy network, heat can be supplied through two main pathways: direct hydrogen combustion and waste heat recovery from the hydrogen fuel cell. In the specific case of Córdoba using N-ethylcarbazole, the hydrogen combustion capacity is set to zero. This result is surprising, since both the hydrogenation and dehydrogenation processes require an input of thermal energy. Under these conditions, the fuel cell remains the sole heat source for the LOHCs system. At first glance, this configuration may appear counterintuitive. Hydrogenation typically occurs during periods of excess electricity generation, when operating the fuel cell for power production would not be expected. However, the results show that during hydrogenation periods, the fuel cell operates at very low load, supplying the required heat for the hydrogenation process (mainly LOHCs preheating), even when surplus renewable electricity is available. This operational strategy can be explained by the proposed economic optimization. The cost of hydrogen combustion is comparatively high, making it less attractive as a heat source. Therefore, when possible, the system relies exclusively on the fuel cell to provide heat, thereby avoiding the additional capital and operational costs associated with installing and operating combustion units. As a result, the fuel cell operates outside the typical storage/production logic, at minimal power output but providing valuable co-generated heat for process integration. This effect is particularly pronounced with N-ethylcarbazole, which requires lower thermal energy input compared to the other analyzed LOHCs system.

Regarding the hydrogenation and dehydrogenation scheme, the hydrogenation process typically takes place during periods of high solar and wind power generation. It overlaps with elevated hydrogen production in the electrolyzer. However, as shown in Figure 5, there are also instances when LOHCs hydrogenation occurs during periods of low electricity generation, for example, around hour 45–50 of the December week. In these situations, there is no hydrogen generation from electrolysis. Instead, part of the compressed hydrogen inventory is redirected to the LOHCs system. This operational strategy allows for more effective management of the available hydrogen, ensuring system flexibility and stable operation. Since the hydrogenation and dehydrogenation processes are not major consumers of electricity, their operation can be scheduled during low-generation hours without significantly affecting the overall power balance.

A comparison between the two LOHCs systems evaluated reveals that the dehydrogenation process capacities for the three provinces are lower when using the indole-based LOHCs system compared to N-ethylcarbazole in spite of lower investment in the first one. Higher dehydrogenation capacities for N-ethylcarbazole are explained due to the lower thermal requirements compared to indoles. It increases the overall energy efficiency of N-ethylcarbazole cycle. This fact is reflected in a higher renewables capacity in the case of indoles, that require to produce a higher amount of hydrogen to supply extra thermal energy demand compared to the other LOHCs system. On the other hand, hydrogenation capacities are higher for indoles. This is attributed to a more intensive use of hydrogenation technology in some specific periods and lower investment compared to N-ethylcarbazole hydrogenation process.

With regards to the storage of total LOHCs material, larger amount is placed for the indole mixture in all cases. This is because N-ethylcarbazole system exhibits higher energy density. In addition, the thermal energy requirements of the hydrogenation and dehydrogenation processes differ between both. As detailed in the model parameters provided in the Supporting Information file, the indole system exhibits higher thermal energy demands, which in turn necessitate larger hydrogen combustion capacities. This underscores the strong interdependence between energy density, process design, and heat integration strategies in the selection and optimization of LOHCs systems.

4.2. Economic results

Based on the design and operational results, an economic evaluation of the integrated power and hydrogen production facility has been carried out. The analysis begins with an assessment of the capital expenditures (CAPEX) associated with the different system components. Figure 7 presents a detailed breakdown of the investment costs for the three selected provinces and for both LOHCs systems evaluated.

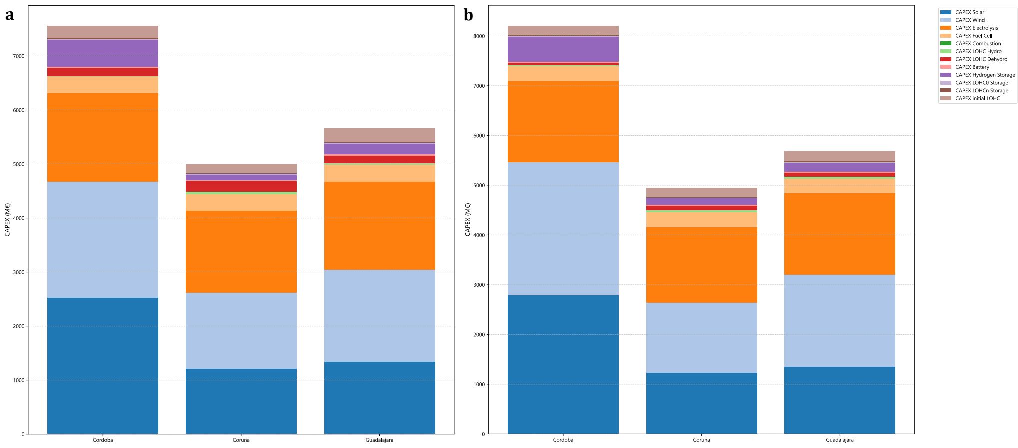

Figure 7: Capital cost breakdown for the two LOHC systems (a - N-ethylcarbazole; b - indoles) and the three selected provinces.

Significant differences in capital investment can be observed among the provinces analyzed, closely linked to the optimized capacity levels presented in the previous section. Power generation technologies, namely onshore wind and photovoltaic solar, account for approximately 55–65% of total capital expenditures. They represent the largest cost component of the integrated energy system. The local availability of wind and solar resources strongly influences the optimized generation capacity and, consequently, the associated capital costs. In Córdoba, where solar energy dominates, the required investment in solar and wind infrastructure reaches nearly 5500 M€, significantly higher than in A Coruña and Guadalajara, where wind generation plays a more prominent role. This difference arises primarily from the lower capacity factor of PV solar, which necessitates a larger oversizing of the installed capacity to meet energy demand, leading to higher capital expenditures. According to the cost parameters used in the optimization model, the current CAPEX values are assumed at 1050 €/kW for solar PV and 1400 €/kW for onshore wind. However, future cost reductions are expected. By 2050, according to Vatankhah Ghadim et al. (2025), these values could decline to 160–630 €/kW for PV solar and 820–1570 €/kW for onshore wind. A more substantial cost decrease is anticipated for photovoltaic technology, which will significantly lower investment needs in provinces with high solar penetration, thereby improving the economic competitiveness of solar-dominated energy systems.

The second largest contributor to CAPEX is hydrogen production through water electrolysis. In this study, a PEM electrolyzer has been considered, with a capital intensity of approximately 1600 €/kW, based on the model parameters. Hydrogen production represents a key bottleneck in the deployment of hydrogen as an energy storage and energy carrier system, with the high capital cost of electrolyzers being one of the main cost drivers of the integrated facility. However, technological advancements are expected to substantially reduce these costs. According to Roeder et al. (2024), the capital cost of PEM electrolysis could decrease to around 670 €/kW by 2050, representing a reduction of more than 50%. This would significantly enhance the economic viability and competitiveness of hydrogen-based energy systems. As shown in Table 4, in all provinces analyzed, the electrolyzer capacity is sized near the upper limit allowed by the optimization model. Consequently, the contribution of electrolyzer CAPEX is similar across locations.

The remaining CAPEX items represent a smaller share of the total investment compared to renewable power generation and electrolysis. Among these, compressed hydrogen storage constitutes the most relevant cost component, particularly in Córdoba, where the required hydrogen storage capacity is significantly higher due to the seasonal profile of solar power generation. In contrast, the LOHCs-based storage system (including hydrogenation and dehydrogenation units, storage tanks, and the initial purchase of the liquid carrier) accounts for only a minor fraction of total capital expenditures. The initial acquisition of the LOHCs represents the largest cost item within this category. Nevertheless, the overall investment required for LOHCs implementation does not represent a major economic barrier to its integration into the energy system. Within the LOHCs processes, dehydrogenation units are more capital-intensive than hydrogenation units. Comparing the two LOHCs systems evaluated (N-ethylcarbazole and an indole mixture) reveals slight differences in initial LOHCs investment. Although a larger mass of the indole mixture is required, the higher unit price of N-ethylcarbazole (2.6 €/kg) relative to the indole mixture (2.0 €/kg) results in a greater initial investment for the N-ethylcarbazole system.

The effect of the cost of energy has also been evaluated in this work to assess the economic performance of the proposed facilities. The results of the operating costs for the installations located in the selected provinces are summarized in Table 5. Two cost indicators were calculated:

- "Demand cost", which considers only the operating cost associated with the electricity and hydrogen demand of the steel plant.
- "Total cost", which accounts for the entire energy production of the system, including the excess electricity generated at each location.

Table 5: Economic results for the two analyzed LOHCs systems (N-ethylcarbazole (LOHC1) and the indoles mixture (LOHC2)) in the selected provinces

	LOHC1			LOHC2		
	Cordoba	**Coruña**	**Guadalajara**	**Cordoba**	**Coruña**	**Guadalajara**
Electricity Excess (%)	389.37	86.78	137.20	475.72	88.31	159.61
% Solar	75.89	43.53	53.20	73.66	44.04	51.43
% Wind	24.11	56.47	46.80	26.34	55.96	48.57
Demand cost (€/MWh)	223.23	158.66	179.98	244.36	158.44	182.25
Total cost (€/MWh)	84.00	115.87	113.62	80.78	115.15	108.52
Energy contribution steel cost (€/t)	722.11	513.23	582.19	790.43	515.51	589.54

To better contextualize these results, the share of wind and solar power generation as well as the magnitude of excess electricity in each province are reported. The high level of excess electricity generation is a critical factor influencing economic profitability. As discussed previously, a considerable fraction of the electricity produced exceeds the plant's demand in all locations analyzed. When the excess generation is not included in the cost calculation, the specific energy cost ranges from 160 to 220 €/MWh, depending on the province. This variation is strongly correlated with the renewable resource mix. For example, Córdoba, characterized by a high share of solar power, exhibits the highest energy cost (about 220 €/MWh). This is mainly driven by the substantial capital investment required to install a large solar PV capacity, necessary to compensate for daily and seasonal variability. Here, power production exceeds the demand by approximately 390%, significantly affecting the cost structure. However, if this surplus electricity were sold, the energy cost could decrease to around 84 €/MWh, representing a notable cost reduction and improving overall economic performance. A similar trend is observed in A Coruña and Guadalajara, although the impact is less pronounced due to the higher share of wind power, which reduces both the magnitude of the surplus and the gap between "Demand cost" and "Total cost". It is important to highlight that this cost comparison is not entirely symmetric. In provinces with greater wind penetration, such as A Coruña and Guadalajara, the installed renewable capacity could be further increased, potentially enabling higher energy production and lower total costs per unit of energy.

However, the integration of surplus electricity must be carefully analyzed to develop effective strategies that enhance the economic viability of these energy systems. One promising approach is the deployment of large-scale energy storage, particularly at the grid level (Sánchez et al., 2022; Calero et al., 2023). Locations with a high share of solar power are especially prone to producing substantial surpluses due to strong seasonal variability, making seasonal storage technologies (hydrogen, methanol, ammonia, LOHCs systems, etc.) a key enabler for balancing supply and demand. Alternatively, the design of the integrated facility could be reconfigured to reduce surplus generation and provide grid support, thereby increasing overall system flexibility. Nonetheless, the economic implications of implementing such storage technologies must be carefully considered to ensure cost-effective operation. Another promising option is the utilization of surplus renewable electricity in the chemical and process industries, which are undergoing deep decarbonization efforts. The electrification of industrial processes has been identified as a viable pathway to reduce emissions (Baldea et al., 2025), and access to low-cost renewable surpluses could significantly reduce operational costs in these sectors. However, to fully exploit this opportunity, a larger operational flexibility is required, as many of these industries have traditionally been designed to operate in steady-state conditions.

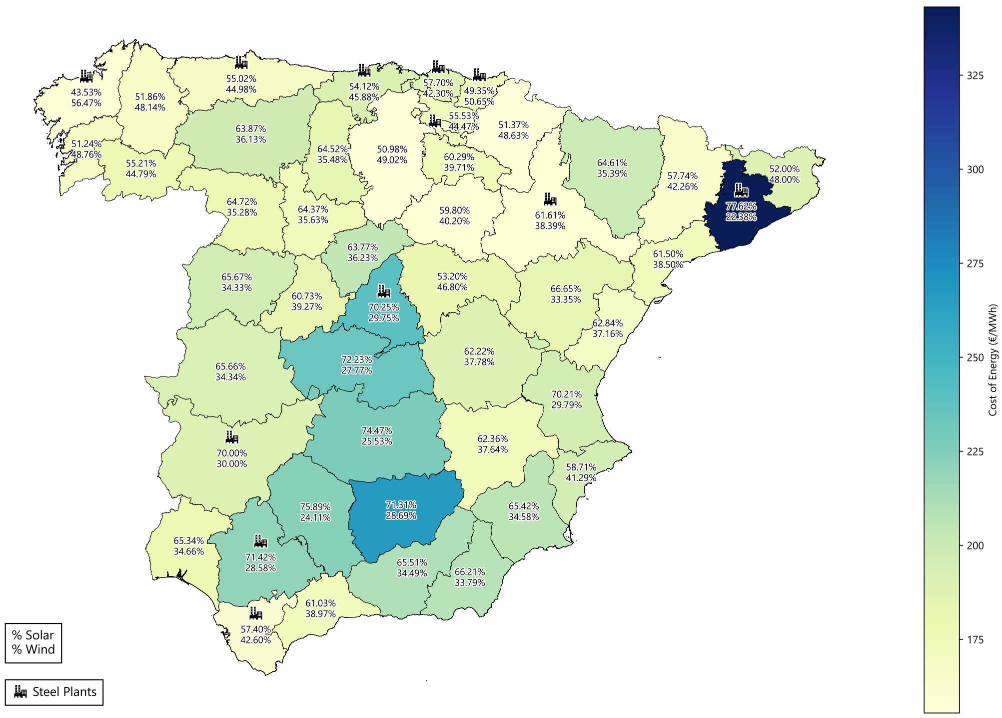

Figure 8: Cost of energy in the different analyzed provinces with the share of wind and solar resources in each facility and the current location of the steel plant with N-ethylcarbazole as LOHC

For comparative purposes, the cost of the proposed green steel production route based on H_2 direct reduction of iron (H_2 DRI) has been benchmarked against conventional steelmaking processes. These include blast furnace–basic oxygen furnace

(BF–BOF) and natural gas–based direct reduction of iron (NG–DRI). The energy consumption associated with each process has been used to calculate the energy cost contribution. Electricity consumption for the reference routes was obtained from Fan and Friedmann (2021) and Rosner et al. (2023), while natural gas and coke consumption were taken from Fan and Friedmann (2021); Rosner et al. (2023) and Safarian (2023), respectively. Natural gas prices (Henry Hub and Russian origin) and coke prices were sourced from Steelonthenet (2025), considering a price range to reflect regional variability. For electricity, a Power Purchase Agreement (PPA) price was assumed in line with Bhaskar et al. (2022). Based on these data, the total energy cost for the BF–BOF route is approximately 17.20 €/MWh, whereas for the NG–DRI route it ranges between 14.97 €/MWh and 36.37 €/MWh, depending on the natural gas price. As expected, these values are significantly lower than the energy costs associated with the renewable-based integrated facility proposed in this work. However, this direct energy cost comparison does not fully capture the differences in energy intensity across the technologies. Notably, the H_2 DRI route exhibits lower specific energy requirements than traditional processes, which influences the cost structure at the product level. To enable a more equitable comparison, the contribution of energy costs to the total steel production cost was evaluated. For the BF–BOF route, this contribution is approximately 113.94 €/ton, whereas for the NG–DRI route, it lies between 48.68 €/ton and 118.22 €/ton. The corresponding results for the H_2 DRI route, summarized in Table 5, show a strong dependence on local renewable resource availability, particularly the balance between solar and wind generation. Although the absolute energy cost for H_2 DRI is higher, the range of variability across provinces is narrower than in the case of pure energy cost, reflecting more consistent energy use per ton of steel. To make the H_2 DRI route economically competitive, cost reductions in key technologies are essential. Predicted declines in the capital costs of renewable power systems and electrolyzers, currently the main economic bottlenecks, are expected to play a critical role. Additionally, CO_2 emission pricing will likely increase the cost of conventional BF–BOF and NG–DRI routes, improving the relative competitiveness of green hydrogen–based steelmaking in the medium to long term.

Finally, to provide a comprehensive overview of all the provinces analyzed and to draw general insights, the electricity cost results ("Demand cost") for the entire set of locations are presented together with the percentage contributions of solar and wind generation in each province. Additionally, the geographical location of existing steel manufacturing facilities in Spain is included. Figure 8 illustrates these results for the N-ethylcarbazole system, whereas Figure 9 presents the corresponding results for the mixture of indoles.

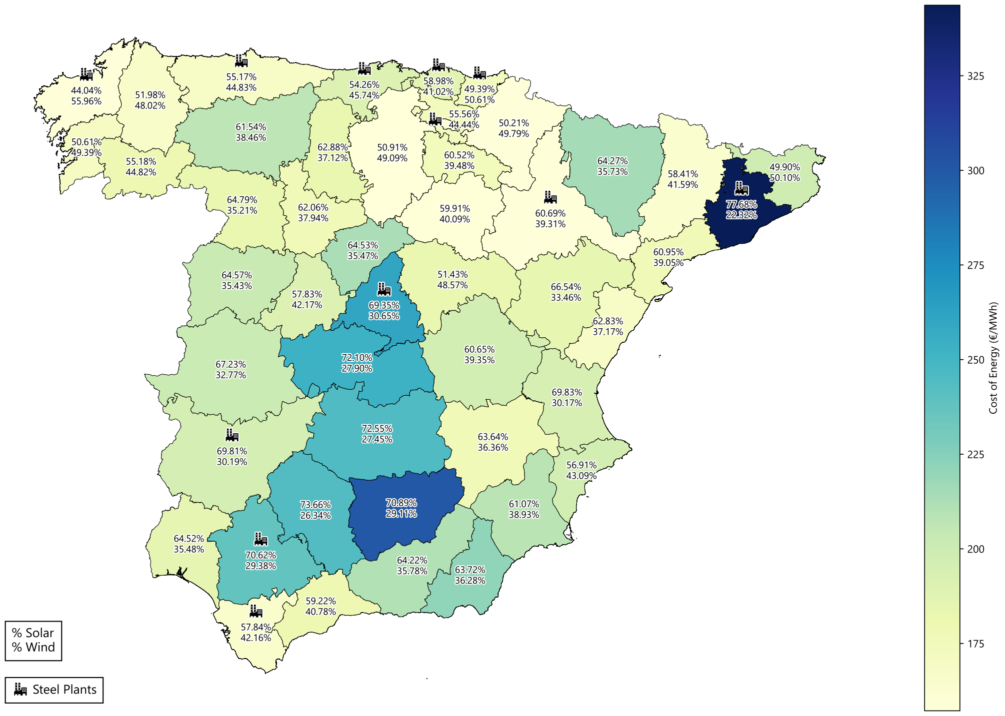

Figure 9: Cost of energy in the different analyzed provinces with the share of wind and solar resources in each facility and the current location of the steel plant with a mixture of indoles as LOHC

As demonstrated in the three representative provinces analyzed, locations where PV solar generation is dominant are consistently associated with higher energy costs. This is mainly attributable to the daily and seasonal variability of solar energy, which necessitates larger installed capacities and consequently increases investment costs. This effect is particularly evident in Barcelona, where PV generation exceeds 75% of total renewable output. It results in electricity costs above 300 €/MWh for both LOHCs systems. When comparing N-ethylcarbazole and indoles system, overall costs are similar, with the second one exhibiting slightly higher average costs. This difference is primarily explained by the higher energy density of N-ethylcarbazole and its lower thermal requirements, which offers economic advantages for this LOHCs system. The spatial distribution of current steelmaking facilities in Spain reveals that some of these plants are located in provinces with medium-to-low projected energy costs, aligning well with the proposed renewable-based facility. However, in other cases (such as Barcelona and Seville) the expected energy costs are significantly higher, raising important considerations regarding future location strategies for green steel production. While repurposing existing steel infrastructure could reduce capital expenditure and facilitate transition pathways, it may also result in higher operational costs in certain regions. Beyond purely economic factors, social and regional development aspects must also be considered. The potential relocation of steel production away from certain provinces could result in job losses and reduced economic activity, particularly in regions with lower population density, where steelmaking has traditionally played a key socioeconomic role.

5. Conclusions

This work proposes a design and scheduling optimization approach to integrate renewable energy into green steel production through the DRI–H_2 process. An integrated energy generation and storage system is assessed to meet the continuous electricity and hydrogen demand of green steel manufacturing. Specifically, two renewable generation technologies (solar photovoltaic and onshore wind) are combined with three storage solutions (batteries, compressed hydrogen, and LOHCs systems). A design and scheduling optimization formulation is developed to determine both the optimal sizing of each unit and the operation strategy of the entire system. A case study for multiple locations (all the mainland provinces) across Spain is conducted to capture the variability in solar and wind resource availability. However, the results from this work can be extrapolated to other regions. Overall, renewable resource availability determines optimal process design and operation. Wind-dominated regions require reduced energy storage capacities, particularly for seasonal storage, compared to solar-dominated areas. Furthermore, the results demonstrate that a combination of energy storage solutions operating at different time horizons is required for effective integration with renewable energy sources. These general insights can be also extrapolated to other sectors integrating renewables with energy storage.

One of the main challenges identified is the large excess of electricity generation, which significantly affects the economic performance of the system. Integrating other final energy consumers or exploring strategies to valorize excess electricity could improve economic profitability. The estimated cost of energy (electricity and hydrogen) ranges on average between 150-250 €/MWh, corresponding to approximately 500–600 € per tonne of steel. Although this remains higher than the cost associated with conventional production routes, future cost reductions in renewable energy generation and electrolysis technologies (the two main bottlenecks) and possible taxes on CO_2 emissions are expected to narrow this gap. Finally, the spatial distribution of current steelmaking facilities in Spain reveals that some plants are located in high-cost energy regions, potentially limiting the reuse of existing infrastructure in a renewable based steel sector. Future research directions include the incorporation of uncertainty in renewable resource availability through stochastic optimization approaches, the evaluation of different steel production scales and their effect on optimal system configuration, the potential interaction with the electricity grid, the analysis of synergies with other industrial hydrogen and energy consumers and the possibility to perform multiobjective optimization within an holistic approach considering economic, environmental and social criteria. Overall, the results demonstrate that proposed integrated network combining generation and storage technologies enables stable electricity and hydrogen supply to green steel plants, providing a viable pathway toward decarbonizing the steel industry.

Nomenclature

BF	Blast furnace
BOF	Basic oxygen furnace
CAPEX	Capital expenditure
EAF	Electric arc furnace
GHG	Greenhouse gases
LOHC	Liquid organic hydrogen carrier
MILP	Mixed integer linear programming
NG	Natural gas
OPEX	Operational expenditure
PEM	Proton exchange membrane
SOFC	Solid oxide fuel cell
B_{jht}	amount of resource consumed
C_i	production capacity for different processes
$D_{j,h,t}$	required demand
J_{imht}	process operating cost not related to capital cost
$\overline{M}$	big-M parameter
OC	Operating cost
$\overline{P}_{imht}$	reference resource produced in certain mode
$\overline{Q}_{jht}$	inventory level
S_{jht}	amount of resource release
x_i	binary variable to select process units
y_{imht}	binary variable to select a mode for a specific process
ρ_{ij}	conversion factor of the different products with respect to the reference resource
η_{iht}	availability of production capacity for wind/solar
$\bar{\Delta}_{im}^{\max}$	maximum rate of change
σ_i	conversion factor between capital and operating cost for a process

δ_i fixed capital cost coefficient
γ_i unit capital cost coefficient
α_j annualized fixed capital cost for storing
β_j annualized unit capital cost for storing
ξ_j O&M cost for storing

Acknowledgments

The authors acknowledge Ministry of Science, Innovation, and Universities Spain grant PID2023-1462310B-I00 and the FPU, Spain grant (FPU21/02413) to C.P.

References

Abdin, Z., Tang, C., Liu, Y., Catchpole, K., 2021. Large-scale stationary hydrogen storage via liquid organic hydrogen carriers. iScience 24, 102966. URL: https://www.sciencedirect.com/science/article/pii/S2589004221009342, doi:https://doi.org/10.1016/j.isci.2021.102966.

Allen, M., Dube, O., Solecki, W., Aragón-Durand, F., Cramer, W., Humphreys, S., Kainuma, M., Kala, J., Mahowald, N., Mulugetta, Y., Perez, R., Wairiu, M., Zickfeld, K., 2018. Framing and context, in: Masson-Delmotte, V., Zhai, P., Pörtner, H.O., Roberts, D., Skea, J., Shukla, P., Pirani, A., Moufouma-Okia, W., Péan, C., Pidcock, R., Connors, S., Matthews, J., Chen, Y., Zhou, X., Gomis, M., Lonnoy, E., Maycock, T., Tignor, M., Waterfield, T. (Eds.), Global Warming of 1.5°C. An IPCC Special Report on the impacts of global warming of 1.5°C above pre-industrial levels and related global greenhouse gas emission pathways, in the context of strengthening the global response to the threat of climate change, sustainable development, and efforts to eradicate poverty. Cambridge University Press, Cambridge, UK and New York, NY, USA, pp. 49–92. doi:10.1017/9781009157940.003.

Allman, A., Palys, M.J., Daoutidis, P., 2019. Scheduling-informed optimal design of systems with time-varying operation: A wind-powered ammonia case study. AIChE Journal 65, e16434. URL: https://aiche.onlinelibrary.wiley.com/doi/abs/10.1002/aic.16434, doi:https://doi.org/10.1002/aic.16434, arXiv:https://aiche.onlinelibrary.wiley.com/doi/pdf/10.1002/aic.16434.

Andersson, J., 2021. Application of liquid hydrogen carriers in hydrogen steelmaking. Energies 14. URL: https://www.mdpi.com/1996-1073/14/5/1392, doi:10.3390/en14051392.

Baldea, M., Endler, E.E., Hale, E., Maravelias, C.T., Barolo, M., Harjunkoski, I., Mercangoz, M., Shah, S.L., Soroush, M., Young, B.R., Zhang, Q., 2025. Transforming the process industries through electrification: Challenges and opportunities. Industrial & Engineering Chemistry Research 64, 16466–16478. doi:10.1021/acs.iecr.5c01256.

Bhaskar, A., Abhishek, R., Assadi, M., Somehesaraei, H.N., 2022. Decarbonizing primary steel production : Techno-economic assessment of a hydrogen based green steel production plant in norway. Journal of Cleaner Production 350, 131339. URL: https://www.sciencedirect.com/science/article/pii/S0959652622009659, doi:https://doi.org/10.1016/j.jclepro.2022.131339.

Bhaskar, A., Assadi, M., Nikpey Somehsaraei, H., 2020. Decarbonization of the iron and steel industry with direct reduction of iron ore with green hydrogen. Energies 13. URL: https://www.mdpi.com/1996-1073/13/3/758.

Bollmann, J., Mitländer, K., Beck, D., Schühle, P., Bauer, F., Zigan, L., Wasserscheid, P., Will, S., 2023. Burner-heated dehydrogenation of a liquid organic hydrogen carrier (lohc) system. International Journal of Hydrogen Energy 48, 30039–30056. URL: https://www.sciencedirect.com/science/article/pii/S0360319923017925, doi:https://doi.org/10.1016/j.ijhydene.2023.04.062.

Calero, F., Cañizares, C.A., Bhattacharya, K., Anierobi, C., Calero, I., de Souza, M.F.Z., Farrokhabadi, M., Guzman, N.S., Mendieta, W., Peralta, D., Solanki, B.V., Padmanabhan, N., Violante, W., 2023. A review of modeling and applications of energy storage systems in power grids. Proceedings of the IEEE 111, 806–831. doi:10.1109/JPROC.2022.3158607.

Climate Action Tracker, 2024. Decarbonising steel-national circumstances and priority actions-august 2024 .

de la Cruz, V., Martín, M., 2016. Characterization and optimal site matching of wind turbines: Effects on the economics of synthetic methane production. Journal of Cleaner Production 133, 1302 – 1311. URL: http://www.sciencedirect.com/science/article/pii/S0959652616306874, doi:https://doi.org/10.1016/j.jclepro.2016.06.019.

Dautel, J.L., Thakur, J., Elberry, A.M., 2024. Enabling industrial decarbonization: A milp optimization model for low-carbon hydrogen supply chains. International Journal of Hydrogen Energy 77, 863–891. URL: https:

//www.sciencedirect.com/science/article/pii/S0360319924022493, doi:https://doi.org/10.1016/j.ijhydene.2024.06.050.

Davis, N.N., Badger, J., Hahmann, A.N., Hansen, B.O., Mortensen, N.G., Kelly, M., Larsén, X.G., Olsen, B.T., Floors, R., Lizcano, G., et al., 2023. The global wind atlas: A high-resolution dataset of climatologies and associated web-based application. Bulletin of the American Meteorological Society 104, E1507–E1525.

Devlin, A., Kossen, J., Goldie-Jones, H., Yang, A., 2023. Global green hydrogen-based steel opportunities surrounding high quality renewable energy and iron ore deposits. Nature Communications 14, 2578.

Elsheikh, H., Eveloy, V., 2022. Assessment of variable solar- and grid electricity-driven power-to-hydrogen integration with direct iron ore reduction for low-carbon steel making. Fuel 324, 124758. URL: https://www.sciencedirect.com/science/article/pii/S0016236122016040, doi:https://doi.org/10.1016/j.fuel.2022.124758.

Elsheikh, H., Eveloy, V., 2023. Renewable hydrogen based direct iron ore reduction and steel making with grid assistance. Energy Conversion and Management 297, 117544. URL: https://www.sciencedirect.com/science/article/pii/S0196890423008907, doi:https://doi.org/10.1016/j.enconman.2023.117544.

European Commission, J., 2025. Photovoltaic geographical information system.

Eveloy, V., Kannan, P., Romeo, L.M., 2024. Comparative energy, emissions and economic assessment of low-carbon iron and steel making processes using imported liquid organic hydrogen carrier options. International Journal of Hydrogen Energy 89, 1321–1341. URL: https://www.sciencedirect.com/science/article/pii/S0360319924040977, doi:https://doi.org/10.1016/j.ijhydene.2024.09.372.

Fan, Z., Friedmann, S.J., 2021. Low-carbon production of iron and steel: Technology options, economic assessment, and policy. Joule 5, 829–862. URL: https://www.sciencedirect.com/science/article/pii/S2542435121000957, doi:https://doi.org/10.1016/j.joule.2021.02.018.

Fuhrlaender, D., Vermeulen, B., Schnuelle, C., 2025. Green hydrogen transformation of the iron and steel production system: An integrated operating concept for system-internal balance, lower emissions, and support for power system stability. Applied Energy 381, 125104. URL: https://www.sciencedirect.com/science/article/pii/S0306261924024887, doi:https://doi.org/10.1016/j.apenergy.2024.125104.

Gambini, M., Guarnaccia, F., Manno, M., Vellini, M., 2024. Feasibility study of lohc-sofc systems under dynamic behavior for cargo ships compared to ammonia alternatives. International Journal of Hydrogen Energy 81, 81–92. URL: https://www.sciencedirect.com/science/article/pii/S0360319924028982, doi:https://doi.org/10.1016/j.ijhydene.2024.07.224.

Germscheid, S.H., Röben, F.T., Sun, H., Bardow, A., Mitsos, A., Dahmen, M., 2023. Demand response scheduling of copper production under short-term electricity price uncertainty. Computers & Chemical Engineering 178, 108394. URL: https://www.sciencedirect.com/science/article/pii/S0098135423002648, doi:https://doi.org/10.1016/j.compchemeng.2023.108394.

Gonzalez-Castellanos, A., Pozo, D., Bischi, A., 2020. Detailed li-ion battery characterization model for economic operation. International Journal of Electrical Power & Energy Systems 116, 105561. URL: https://www.sciencedirect.com/science/article/pii/S0142061519315765, doi:https://doi.org/10.1016/j.ijepes.2019.105561.

Griffiths, S., Sovacool, B.K., Kim, J., Bazilian, M., Uratani, J.M., 2021. Industrial decarbonization via hydrogen: A critical and systematic review of developments, socio-technical systems and policy options. Energy Research & Social Science 80, 102208. URL: https://www.sciencedirect.com/science/article/pii/S2214629621003017, doi:https://doi.org/10.1016/j.erss.2021.102208.

Hlal, M.I., Ramachandaramurthy, V.K., Sarhan, A., Pouryekta, A., Subramaniam, U., 2019. Optimum battery depth of discharge for off-grid solar pv/battery system. Journal of Energy Storage 26, 100999. URL: https://www.sciencedirect.com/science/article/pii/S2352152X19305286, doi:https://doi.org/10.1016/j.est.2019.100999.

Immonen, J., Weingaertner, D., Ketkaew, J., Prasher, R., Powell, K.M., 2025. Process intensification and comparison of electrolytic hydrogen green steel plants for industrial decarbonization. Journal of Cleaner Production 490, 144812. URL: https://www.sciencedirect.com/science/article/pii/S0959652625001623, doi:https://doi.org/10.1016/j.jclepro.2025.144812.

International Energy Agency, 2020. Iron and steel technology roadmap. https://www.iea.org/reports/iron-and-steel-technology-roadmap. IEA, Paris. Licence: CC BY 4.0.

International Energy Agency, 2021. Net zero by 2050. https://www.iea.org/reports/net-zero-by-2050. IEA, Paris. Licence: CC BY 4.0.

Jeong, Y., Zhang, Q., 2025. Transition toward a decarbonized steel industry: A supply chain analysis for the united states. Industrial & Engineering Chemistry Research 64, 16263–16280. doi:10.1021/acs.iecr.5c01586.

Kebede, A.A., Kalogiannis, T., Van Mierlo, J., Berecibar, M., 2022. A comprehensive review of stationary energy storage devices for large scale renewable energy sources grid integration. Renewable and Sustainable Energy Reviews 159, 112213. URL: https://www.sciencedirect.com/science/article/pii/S1364032122001368, doi:https://doi.org/10.1016/j.rser.2022.112213.

Lin, A., Bagnato, G., 2024. Revolutionising energy storage: The latest breakthrough in liquid organic hydrogen carriers. International Journal of Hydrogen Energy 63, 315–329. URL: https://www.sciencedirect.com/science/article/pii/S0360319924009789, doi:https://doi.org/10.1016/j.ijhydene.2024.03.146.

Narayanan, T.M., He, G., Gençer, E., Shao-Horn, Y., Mallapragada, D.S., 2022. Role of liquid hydrogen carriers in deeply decarbonized energy systems. ACS Sustainable Chemistry & Engineering 10, 10768–10780. doi:10.1021/acssuschemeng.2c00909.

Niermann, M., Beckendorff, A., Kaltschmitt, M., Bonhoff, K., 2019. Liquid organic hydrogen carrier (lohc) – assessment based on chemical and economic properties. International Journal of Hydrogen Energy 44, 6631–6654. URL: https://www.sciencedirect.com/science/article/pii/S0360319919303581, doi:https://doi.org/10.1016/j.ijhydene.2019.01.199.

Pawelec, G., Fonseca, J., 2022. Steel from solar energy: A techno-economic assessment of green steel manufacturing. Hydrogen Europe, Brussels, Belgium .

Peters, R., Deja, R., Engelbracht, M., Frank, M., Nguyen, V.N., Blum, L., Stolten, D., 2016. Efficiency analysis of a hydrogen-fueled solid oxide fuel cell system with anode off-gas recirculation. Journal of Power Sources 328, 105–113. URL: https:

//www.sciencedirect.com/science/article/pii/S0378775316310011, doi:https://doi.org/10.1016/j.jpowsour.2016.08.002.

Preuster, P., Fang, Q., Peters, R., Deja, R., Nguyen, V.N., Blum, L., Stolten, D., Wasserscheid, P., 2018. Solid oxide fuel cell operating on liquid organic hydrogen carrier-based hydrogen – making full use of heat integration potentials. International Journal of Hydrogen Energy 43, 1758–1768. URL: https://www.sciencedirect.com/science/article/pii/S0360319917343719, doi:https://doi.org/10.1016/j.ijhydene.2017.11.054.

Prieto, C., Sánchez, A., Martín, M., 2025. A two-step methodology for the selection and process optimization of liquid organic hydrogen carriers (lohcs). International Journal of Hydrogen Energy 135, 69–85. URL: https://www.sciencedirect.com/science/article/pii/S0360319925020580, doi:https://doi.org/10.1016/j.ijhydene.2025.04.371.

Rasul, M., Hazrat, M., Sattar, M., Jahirul, M., Shearer, M., 2022. The future of hydrogen: Challenges on production, storage and applications. Energy Conversion and Management 272, 116326. URL: https://www.sciencedirect.com/science/article/pii/S0196890422011049, doi:https://doi.org/10.1016/j.enconman.2022.116326.

Roeder, T., Rosenstiel, A., Monnerie, N., Sattler, C., 2024. Impact of expected cost reduction and lifetime extension of electrolysis stacks on hydrogen production costs. International Journal of Hydrogen Energy 95, 1242–1251. URL: https://www.sciencedirect.com/science/article/pii/S0360319924031641, doi:https://doi.org/10.1016/j.ijhydene.2024.08.015.

Rosner, F., Papadias, D., Brooks, K., Yoro, K., Ahluwalia, R., Autrey, T., Breunig, H., 2023. Green steel: design and cost analysis of hydrogen-based direct iron reduction. Energy Environ. Sci. 16, 4121–4134. URL: http://dx.doi.org/10.1039/D3EE01077E, doi:10.1039/D3EE01077E.

Safarian, S., 2023. To what extent could biochar replace coal and coke in steel industries? Fuel 339, 127401. URL: https://www.sciencedirect.com/science/article/pii/S0016236123000145, doi:https://doi.org/10.1016/j.fuel.2023.127401.

Schrotenboer, A.H., Veenstra, A.A., uit het Broek, M.A., Ursavas, E., 2022. A green hydrogen energy system: Optimal control strategies for integrated hydrogen storage and power generation with wind energy. Renewable and Sustainable Energy Reviews 168, 112744. URL: https:

//www.sciencedirect.com/science/article/pii/S1364032122006323, doi:https://doi.org/10.1016/j.rser.2022.112744.

Shahabuddin, M., Brooks, G., Rhamdhani, M.A., 2023. Decarbonisation and hydrogen integration of steel industries: Recent development, challenges and technoeconomic analysis. Journal of Cleaner Production 395, 136391. URL: https://www.sciencedirect.com/science/article/pii/S0959652623005498, doi:https://doi.org/10.1016/j.jclepro.2023.136391.

Sinnott, R., Towler, G., 2019. Chemical engineering design: SI Edition. Butterworth-Heinemann.

Steelonthenet, 2025. Raw materials & energy price data. monthly price trends: Iron ore, coal, gas & electricity. URL: https://www.steelonthenet.com/commodity-prices.html.

Stolte, M., Bourig, A., Minuto, F.D., Lanzini, A., 2026. Energy-system optimization for hydrogen-based green steel production from medium-grade iron ore. Applied Energy 410, 127563. URL: https://www.sciencedirect.com/science/article/pii/S0306261926002151, doi:https://doi.org/10.1016/j.apenergy.2026.127563.

Svitnič, T., Sundmacher, K., 2022. Renewable methanol production: Optimization-based design, scheduling and waste-heat utilization with the fluxmax approach. Applied Energy 326, 120017. URL: https://www.sciencedirect.com/science/article/pii/S0306261922012740, doi:https://doi.org/10.1016/j.apenergy.2022.120017.

Sánchez, A., Martín, M., 2018. Optimal renewable production of ammonia from water and air. Journal of Cleaner Production 178, 325 – 342. URL: http://www.sciencedirect.com/science/article/pii/S0959652617332730, doi:https://doi.org/10.1016/j.jclepro.2017.12.279.

Sánchez, A., Zhang, Q., Martín, M., Vega, P., 2022. Towards a new renewable power system using energy storage: An economic and social analysis. Energy Conversion and Management 252, 115056. URL: https://www.sciencedirect.com/science/article/pii/S0196890421012322, doi:https://doi.org/10.1016/j.enconman.2021.115056.

Toktarova, A., Göransson, L., Johnsson, F., 2021. Design of clean steel production with hydrogen: Impact of electricity system composition. Energies 14. doi:10.3390/en14248349.

Vatankhah Ghadim, H., Haas, J., Breyer, C., Gils, H.C., Read, E.G., Xiao, M., Peer, R., 2025. Are we too pessimistic? cost projections for solar photovoltaics, wind power, and batteries are over-estimating actual costs globally. Applied Energy 390, 125856. URL: https://www.sciencedirect.com/science/article/pii/S0306261925005860, doi:https://doi.org/10.1016/j.apenergy.2025.125856.

Vogl, V., Åhman, M., Nilsson, L.J., 2018. Assessment of hydrogen direct reduction for fossil-free steelmaking. Journal of Cleaner Production 203, 736–745. URL: https://www.sciencedirect.com/science/article/pii/S0959652618326301, doi:https://doi.org/10.1016/j.jclepro.2018.08.279.

Yadav, D., Guhan, A., Biswas, T., 2021. Greening Steel: Moving to Clean Steelmaking Using Hydrogen and Renewable Energy: Report. Council on Energy, Environment and Water.

Zhang, Q., Grossmann, I.E., Heuberger, C.F., Sundaramoorthy, A., Pinto, J.M., 2015. Air separation with cryogenic energy storage: Optimal scheduling considering electric energy and reserve markets. AIChE Journal 61, 1547–1558. URL: https://aiche.onlinelibrary.wiley.com/doi/abs/10.1002/aic.14730, doi:https://doi.org/10.1002/aic.14730, arXiv:https://aiche.onlinelibrary.wiley.com/doi/pdf/10.1002/aic.14730.

Zhang, Q., Sundaramoorthy, A., Grossmann, I.E., Pinto, J.M., 2016. A discrete-time scheduling model for continuous power-intensive process networks with various power contracts. Computers & Chemical Engineering 84, 382–393. URL: https://www.sciencedirect.com/science/article/pii/S0098135415003142, doi:https://doi.org/10.1016/j.compchemeng.2015.09.019.